[7] Mihlfeith, C. M., Baer, A. D. and Ryan, N. W., "Propellant Combustion Instability as Measured by Combustion Recoil," *AIAA Journal*, Vol. 10, No. 10, Oct. 1972, pp. 1280–1285.

[8] Thompson, C. L. and Suh, N. P., "The Interaction of Thermal Radiation and M-2 Double Base Propellant," *Combustion Science and Technology*, Vol. 2, No. 1, Jan. 1970, pp. 59.

[9] Kubota, N., Ohlemiller, T. J., Caveny, L. H., and Summerfield, M., "The Mechanism of Super-Rate Burning of Catalyzed Double Base Propellants," Rept. AMS 1087 (AD 763-786), March 1973, Dept. of Aerospace and Mechanical Sciences, Princeton University, Princeton, N.J.

[10] Caveny, L. H., Summerfield, M., and May, I. W., "Propellant Optical Properties and Ignition Characteristics as Modified by Particulate Carbon," AIAA Paper 75-231, Pasadena, Calif., 1975.

FEBRUARY 1975 AIAA JOURNAL VOL. 13, NO. 2

Sensitivity of Laser Absorption Wave Formation to Nonequilibrium and Transport Phenomena

M. R. STAMM* AND P. E. NIELSEN†
Air Force Weapons Laboratory, Kirtland Air Force Base, N. Mex.

Experiments have shown that laser absorption waves (LAW's) may be ignited in air from aerosols or solid surfaces at laser intensities below the clean air breakdown threshold. We present detailed numerical calculations of the formation and structure of such LAW's made with a two-temperature, Lagrangian hydrodynamic computer program containing a fully coupled nonequilibrium breakdown chemistry, electron diffusion, and radiation transport. The detailed LAW structure is then interpreted to delineate the roles of the nonequilibrium, radiative, and transport processes in various regimes.

Nomenclature

c = velocity of light = 3×10^{10} (cm sec^{-1})
ΔE = $I_1 - I_2$
e = electron charge (esu)
f = laser flux (W cm^{-2})
$I_1(I_2)$ = ionization energy of the ground (first excited) state (ev)
I = $4\pi e^2/mc\omega^2 \simeq 2 \times 10^{-11}$ (ev cm^2 watt^{-1}) for $\hbar\omega$ = 0.12 ev
$m(M)$ = electron (atom) mass (gm)
n = electron number density (cm^{-3})
$N = N_1 + N_2 + n$ = total number of heavy particles (cm^{-3})
$N_1(N_2)$ = number density of atoms in the ground (first excited) state (cm^{-3})
$N_n = N_1 + N_2$ = total number of neutral particles (cm^{-3})
P = pressure (erg cm^{-3})
$R_a(T_g)$ = electron attachment rate = $\begin{cases} 1.7 \times 10^{-12} N(n-1) \text{ (Ref. 1)} & T_g < 0.4 \text{ ev} \\ 0 & T_g \geqq 0.4 \text{ ev} \end{cases}$
$R_{i1}(R_{i2})$ = electron impact ionization rate from the ground (first excited) state $\simeq \bar{v}_{i1} \exp(-I_1/T_e)[\bar{v}_{i2} \exp(-I_2/T_e)]$ (Ref. 2)
R_r = radiative recombination rate $\simeq 1.3 \times 10^{-13} T_e^{-1/2}$ (Ref. 2)
R_x = electron impact excitation rate $\simeq 1.6 \times 10^{-8} \exp(-\Delta E/T_e)$ (Refs. 3, 4)
$\bar{R}_x, \bar{R}_{i1}, \bar{R}_{i2}$ = inverse rates of R_x, R_{i1}, R_{i2} from detailed balancing
$T_e(T_g)$ = electron (gas) temperature (ev)
$\bar{v}_{ei}(\bar{v}_{en})$ = electron ion (neutral) elastic collision rate $3.0 \times 10^{-6} T_e^{-3/2}(1.3 \times 10^{-7} T_e^{1/2})$ (Refs. 2, 4)
$\bar{v}_{i1}(\bar{v}_{i2})$ = electron impact ionization rates from ground (first excited) states $\bar{v}_{i1} \simeq 10^{-3}$ (cm^2 sec^{-1}) (Refs. 2, 5) $\bar{v}_{i2} \simeq 3.2 \times 10^{-7}$ (cm^2 sec^{-1}) (Ref. 2)
α = $\bar{v}_{i1} N_1$
β = $(Lf\bar{v}_{en}/\Delta E \bar{v}_x)^{I_1/\Delta E}$
γ = specific heat ratio = C_p/C_v
δ = $(1+\phi)\bar{v}_{en} N_1 I f/(I_1 + \phi I_2)$
θ = $\bar{v}_{i1}/\bar{v}_x$
ϕ = $\bar{v}_{i1}/\bar{v}_{i2}$
ρ = density (g cm^{-3})
σ = photoionization cross section in nitrogen, $\simeq 8 \times 10^{-18}$ cm^2 (Ref. 2)
ω = laser frequency (sec^{-1})

Introduction

COLD clean air breaks down at a threshold CO_2 laser flux of a few times 10^9 W/cm^2,[6,7] but it has been found that in the presence of either solid surfaces or aerosols it may break down in fluxes considerably lower than the clean air breakdown threshold. Once formed, the resulting plasmas may be maintained by fluxes as low as a few times 10^4 W/cm^2.[8,9] These plasmas, which propagate up the beam at well-defined velocities, are called laser supported absorption waves, or "LAW's." The evolution of such LAW's may be divided into three consecutive phases: ignition, formation, and maintenance, each of which is, at present, better understood than the last. These phases refer respectively to the detailed evolution of the solid target material into a plasma, the formation of a LAW in the air ahead of this plasma, and its steady-state propagation in air up the laser beam.

Presented as Paper 74-229 at the AIAA 12th Aerospace Sciences Meeting, Washington, D.C., Jan. 30–Feb. 1, 1974; submitted Feb. 14, 1974; revision received July 15, 1974.

Index categories: Lasers; Plasma Dynamics and MHD.

* Physicist, Theoretical Branch; presently at ARL/LU, Plasma Physics Research Laboratory, Aerospace Research Laboratories, Wright-Patterson Air Force Base, Ohio.

† Chief, Interaction Physics Group, Theoretical Branch; presently at Department of Physics, Air Force Institute of Technology, Wright-Patterson Air Force Base, Ohio.

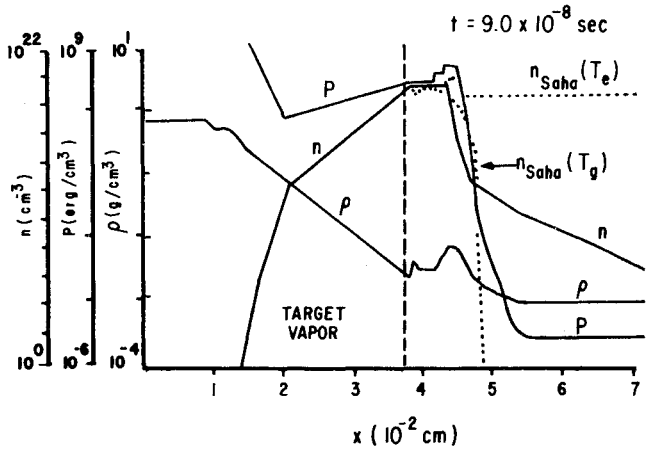

Fig. 1 P, n, and ρ profiles in a LAW.

There have been a number of computer programs[10,11] modeling LAW formation and maintenance which make the assumptions that the electron and gas temperatures, T_e and T_g, are equal or that electron number density, n, is the Saha equilibrium number density at the electron or gas temperatures. Our purpose has been to make detailed numerical calculations of the formation and structure of such LAW's using separate electron and gas temperatures and a nonequilibrium electron number density to determine to what extent and in what regimes such equilibrium models are good approximations, and also to determine the mechanisms primarily responsible for LAW formation.

Our calculations show that before the LAW is formed, and also ahead of an established LAW, the electron temperature is generally higher than the gas temperature. Within this nonequilibrium region, the electron number density is in general less than the Saha equilibrium number density at the electron temperature, $n_{\text{Saha}}(T_e)$, but higher than n_{Saha} at the gas temperature. Once the LAW is established, that is, once $n \geqq 10^{17}$ cm^{-3}, $T_g \simeq T_e$ and $n \simeq n_{\text{Saha}}(T_e)$. In addition, they show that transport processes (e.g., electron diffusion and radiation transport) provide separate mechanisms independent of shock heating for the formation of LAW's, and that they may indeed form LAW's at fluxes too low to provide formation by shock heating.

The Computer Program

These calculations have been made with a one-dimensional, Lagrangian hydrodynamic computer program with separate electron and gas temperatures. Additional effects included are electron ambipolar diffusion and the emission and bound-free absorption of continuum radiation. The main feature of this program is that it contains a simple breakdown chemistry fully coupled to the hydrodynamics.

Our breakdown chemistry treats an idealized two level monatomic gas which may be either in its ground state, first excited state, or singly ionized, as represented by level populations N_1, N_2, and n. The electrons have a temperature T_e, and the heavy particles a temperature T_g. After each hydrodynamic time step the following differential equations are solved to compute changes in T_e, T_g, N_1, N_2, and n resulting from elastic, inelastic, and superelastic collisions between electrons and heavy particles, electron impact ionization and recombination, and free-free absorption of the laser flux in the field of ions and neutrals. These updated values then drive the hydrodynamics on the next step.

$$1.5d/dt(nT_e) = Lf(\bar{\nu}_{en}N_n + \bar{\nu}_{ei}n)n - \Delta E(R_xN_1 - \bar{R}_xN_2)n - I_1(R_{i1}N_1 - \bar{R}_{i1}n^2)n - I_2(R_{i2}N_2 - \bar{R}_{i2}n^2) - (T_e - T_g)(m/M)(\bar{\nu}_{en}N_n + \bar{\nu}_{ei}n)n \quad (1)$$

$$d/dt(NT_g) = (T_e - T_g)(m/M)(\bar{\nu}_{en}N_n + \bar{\nu}_{ei}n)n + Ra(T_g)T_e \quad (2)$$

$$\dot{N}_1 = -(R_xN_1 - \bar{R}_xN_2)n - (R_{i1}N_1 - \bar{R}_{i1}n^2)n \quad (3)$$

$$\dot{N}_2 = +(R_xN_1 - \bar{R}_xN_2)n - (R_{i2}N_2 - \bar{R}_{i2}n^2)n \quad (4)$$

$$\dot{n} = -(\dot{N}_1 + \dot{N}_2) - R_a(T_g) = (R_{i1}N_1 - \bar{R}_{i1}n^2)n + (R_{i2}N_2 - \bar{R}_{i2}n^2)n - R_a(T_g) \quad (5)$$

In addition, it contains a simple model for the attachment of electrons to 0 and 0_2, which may be switched on for "air" calculations, in which the net attachment rate $R_a(T_g)$ is taken to be constant for gas temperatures less than some threshold temperature, typically on the order of a few tenths of an electron volt, and zero otherwise. The flux of continuum radiation is calculated in a single pass from the inner to the outer hydrodynamic cells. It is augmented in each cell by $R_r n^2$ due to radiative recombination, attenuated by $\exp(-\sigma N_1\, dx)$ due to photoionization, as well as being attenuated geometrically. It has been found that, within the framework of this model, line radiation transport has little effect on LAW structure for the cases presented, and has not been included.

Typical LAW Profile

Figures 1 and 2 show the spatial profiles of pressure P, density ρ, n, T_e, and T_g for a typical LAW as predicted by this program. A laser flux of 3×10^7 W/cm^2 coming in from the right has ignited a LAW in "air," shown to the right of the dotted lines, from a slab of target material initially 50 μ thick, shown to the left of the dotted lines. Here "air" is monatomic nitrogen with a temperature of 300°K, a density of 2.9×10^{-3} g cm^{-3}, and with the attachment included. Looking from right to left, we note that a few hundred microns ahead of the front there are few electrons, even though these electrons are at about 1.5 ev, a temperature established in the electron gas by the balance of energy gained by inverse Bremsstrahlung and lost in electron impact excitation. The increasing n approaching the front results from preionization by continuum radiation at distances of a few hundred microns and diffusion at distances of a few tens of microns. At 530 μ, in Figs. 1 and 2, the gas temperature begins to rise due to shock heating, and at 440 μ the electron number density is roughly 10^{19} cm^{-3}, strongly attenuating the beam. Until the beam is attenuated, T_e and T_g cannot equilibrate since continued absorption of the laser flux drives T_e upward, while T_g lags behind, being coupled only weakly to the electrons, primarily by elastic collisions [Eq. (2)]. Here the absorption length is about 30 μ. Once the flux is attenuated, the high n permits rapid equilibration of T_e and T_g by elastic collisions over a length which can be estimated by multiplying the equilibration time by the LAW velocity, giving an equilibration length of about 100 μ. Thus at 430 μ the flux is reduced by an order of magnitude and at 390 μ $T_g \simeq T_e$. Dotted lines show n_{Saha} at T_e and T_g. We see that, ahead of the LAW and within its nonequilibrium region, $n_{\text{Saha}}(T_g) < n < n_{\text{Saha}}(T_e)$; but after about the first 100 μ of the LAW, n reaches the Saha equilibrium number density at either temperature.

The electron temperature profile for this LAW, in which $T_e \simeq 1$ eV ahead of the shock and $T_e > T_g$ within the nonequilibrium region, is in sharp contrast to the temperature profiles for a shock in the absence of a laser flux, where both

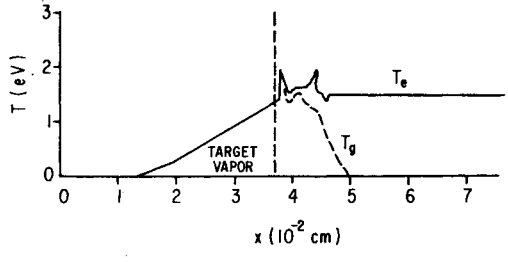

Fig. 2 T_e and T_g profiles in a LAW.

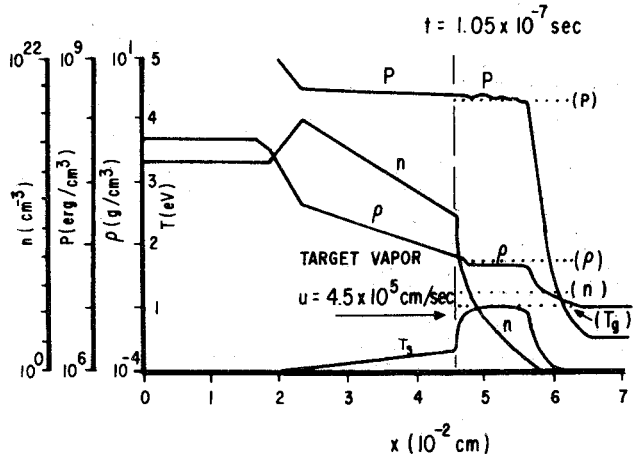

Fig. 3 LAW formation by shock heating alone.

T_e and T_g rise abruptly from ambient values as the shock passes and then reach constant values with $T_e < T_g$.[12] This is because, in the first case, the T_e is established both within and ahead of the nonequilibrium region by the balance between electron energy gained by inverse Bremsstrahlung and lost by electron impact excitation. That is, the laser absorption and electronic excitation terms dominate the right side of Eq. (1), balancing at some T_e such that $\dot{T}_e = 0$. In the second case, however, T_e is set within the nonequilibrium region by the balance between energy gained by elastic collisions and lost to electron impact ionizations. Thus, in this case, the third, fourth and fifth terms dominate Eq. (1). These balance at some other T_e for which $\dot{T}_e = 0$.

LAW Formation

We now consider the roles that the various mechanisms play in initiating a LAW. We observe that, according to Eq. (1), a particular laser flux f establishes a unique steady-state electron temperature T_e via the rates R_{i1}, R_{i2}, R_x, and their inverses. The threshold flux f_o for clean air breakdown establishes a temperature T_{eo} at which the ionization rate in Eq. (5) is slightly greater than the attachment rate.[6] Therefore, f_o may be lowered by decreasing the attachment rate $R_a(T_g)$. We further observe that, according to Eq. (1), f_o is nearly independent of n for $n < (\bar{\nu}_{en}/\bar{\nu}_{ei})N_n \simeq 0.01\ N$. However, once the ionization reaches a few percent, electron-ion collisions predominate over the electron-neutral collisions, and f_o drops linearly with increasing n. Thus we can initiate cascading in air by either heating T_g above T_a and lowering $R_a(T)$, for example by shock heating the gas, or by increasing the n above $\simeq 0.01N$ by preionization.

Shock Heating

The effect of shock heating alone on the formation of a LAW is shown in Fig. 3, in which the initial conditions are the same as in Figs. 1 and 2, except that continuum radiation and diffusion have been turned off. We see that after about the same time, the electron number density in the shock heated gas in front of the expanding target vapor is much lower than before, and that no LAW has yet formed. Whether or not it will depends on how long the gas remains shock heated. Should it form, its profile will resemble that in Figs. 1 and 2, except that the high electron number density in front of the LAW, which owes to preionization, will be absent. The values for P, ρ and T_g within the shock heated region of Fig. 3 are well approximated by the P, ρ and T of a classical piston driven shock,[13] results of which for a piston velocity of 4.5×10^5 cm/sec are shown in dotted lines. An estimate of $n(t)$ in such a shock heated region where $R_a(T_g) = 0$ may be obtained by making certain approximations to Eqs. (1) and (5) and then integrating Eq. (5) directly (see Appendix). This analytic model, when applied to the shock heated gas of Fig. 3, predicts an electron number density of 8.9×10^5 cm^{-3} for a flux of 3×10^7 W/cm^2 after a time of 1.05×10^{-7} sec, which is shown in that figure in dotted lines. If this target were to continue to heat the gas for 3×10^{-7} sec in this flux, then breakdown would occur and a LAW would form due to shock heating alone.

Continuum Radiation and Diffusion

A comparison of the n in Figs. 1–3 shows the considerable effect that the transport mechanisms have on LAW formation. We have also done similar runs in which only ambipolar diffusion or continuum radiation were operative, the shock heating being minimized by beginning the calculation with a hot plasma at ambient pressure. In each case, after the target had time to deposit sufficient electrons in the surrounding air, a LAW was formed. The calculations shown in Fig. 4 dramatically illustrate the fact that either of these two mechanisms can ignite a LAW, by comparing the shock trajectories of LAW's which are formed in one case primarily by shock heating, and in the second case by transport effects alone. It shows time histories of the radius, r (solid lines), and velocity, v (dashed lines), of the shock produced by a 10-ev spherical plasma with an initial radius of 5 μ and an initial density of 1.3×10^{-3} g/cm^3 expanding into a background gas with the same density and a temperature of 300°K. The lowest solid curve (labeled flux = 0) shows the shock trajectory with the laser flux off. The lowest dotted line is the corresponding velocity which, after an initial rise, decreases, approximating the well-known $t^{-3/5}$ behavior of a point explosion,[13] until the speed of sound is reached at 10^{-7} sec. Incident fluxes below 10^7 W/cm^2 do not ignite LAW's within 10^{-6} sec and therefore produce essentially the same results. Higher fluxes, on the other hand, do ignite LAW's. The velocity curve labeled 3×10^8 W/cm^2 shows that under such a flux the leading edge of the plasma is accelerated after 10^{-9} sec as it evolves into an optically thick LAW with a constant velocity $v \simeq [2(\gamma^2-1)f/\rho_o]^{1/3} \simeq 1.5 \times 10^6$ cm/sec, as predicted by Raizer.[14] By contrast, if the flux is an order of magnitude lower, the shock decays into a sonic disturbance and no LAW is formed from it. However, the hot plasma core continues to deposit electrons in the surrounding air via radiation and diffusion, which cascade, forming a LAW which moves out through the decaying shock (the ionization wave is shown in dots), and again quickly reaches the velocity predicted by Raizer.

Conclusions

We therefore conclude that since the equilibration length of a LAW ($\simeq 100$ μ) is much smaller than a typical beam radius (0.1 cm $< r <$ 10 cm), equilibrium models adequately describe the

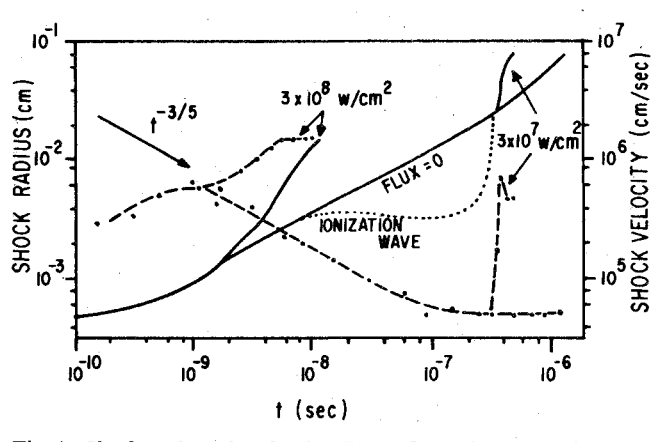

Fig. 4 Shock trajectories showing LAW formation under fluxes of 3×10^7 and 3×10^8 W/cm^2.

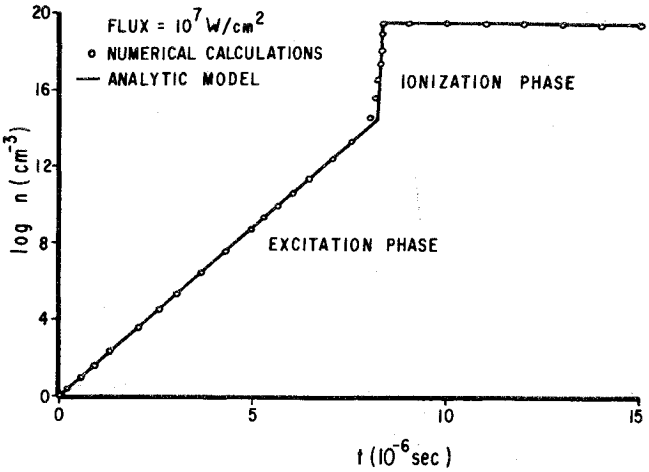

Fig. 5 Electron cascading in a monatomic gas with $N = 3 \times 10^{19}$ cm^{-3} and $R_a(T_g) = 0$.

propagation of LAW's that have already formed. However, during the early ignition and growth phase of a LAW from a target surface, or especially from a small absorbing center, not only is the scale of the problem much smaller, but, because of the low electron number density, the equilibration length is much larger. Thus nonequilibrium effects are crucial for the proper prediction of the ignition of LAW's, especially from small particles.

We further conclude that there are two distinct classes of mechanisms that can initiate LAW formation; namely shock heating and transport mechanisms, and that either of these may predominate depending on the flux and initial conditions. However, once the LAW is established, shock heating becomes the principal mechanism for LAW maintenance. Our future efforts will be directed toward establishing criteria for such ignition and its scaling on laser frequency and ambient pressure.

Appendix: Analytic Breakdown Model

A good analytic approximation to $n(t)$ due to cascading in a gas for which $R_a(T_g) = 0$ results from dividing the breakdown time into two phases. During the first phase, a steady state T_e is established in Eq. (1) with excitations dominant among the loss processes. An approximate T_e may then be found analytically by equating the electron excitation and laser absorption terms and solving for T_e via the rate R_x (see nomenclature). This T_e then defines the rates R_{i1} and R_{i2} so that Eq. (5) can be integrated directly for $n(t)$ in terms of n_o, the initial electron number density, $n(t) = n_o e^{\alpha\beta t}$. Ionization continues at this rate until the ground and first excited state number densities equilibrate at $N_2 = N_1 \exp(-\Delta E/T_e)$, and electron energy losses due to impact excitation are balanced by gains from deexcitation (superelastic collisions). At this time, $t_1 = (\alpha\beta)^{-1} \times \ln(\theta\beta N_1/n_o + 1)$, where n has a value $n(t_1) = n_o + \theta\beta N_1$. (Note: α, β, θ, etc., are defined in the Nomenclature.)

During the second phase, inverse Brehsstrahlung is balanced primarily against electron impact ionization. Equating these terms in Eq. (1) results in a higher T_e, so that the electron number density now grows at a faster rate given by $n(t) = n(t_1)e^{\delta t}$. This continues until $n \simeq N$ after a time $t_2 \simeq \delta^{-1} \ln[N_1/n_1(t_1)]$. For gases at ambient temperature and pressure $t_2 \ll t_1$. The total breakdown time, $t_B = t_1 + t_2$, depends only weakly on n_o, so that the gas breakdown time is insensitive to the initial ionization. For example, increasing n_o from 1 to 10^3 in a typical calculation decreases the breakdown time by only about 20%.

The resulting $n(t)$ for a two level gas with $N_1 = 3 \times 10^{19}$ cm^{-3}, $I_1 = 15$ ev, $I_2 = 3.75$ ev, $R_a(T_g) = 0$, and $n_o = 1$ in a CO_2 laser flux of 10^7 W/cm^2, is shown in Fig. 5 in solid lines. It compares well with the numerical results of the computer program's breakdown chemistry for a similar problem, shown in circles.

References

[1] Kroll, N. and Watson, K. M., "Theoretical Study of Ionization of Air by Intense Laser Pulses," *The Physical Review A*, Vol. 5, No. 4, April 1972, pp. 1883–1905.

[2] Zel'dovich, Ya. B., and Raizer, Yu. P., *Physics of Shock Waves and High-Temperature Hydrodynamic Phenomena*, Vols. 1 and 2, Academic Press, New York, 1967.

[3] Lowke, J. J., Phelps, A. V., and Irwin, B. W., "Predicted Electron Transport Coefficients and Operating Characteristics of CO_2-N_2-He Laser Mixtures," 1973, Westinghouse Research Laboratories Rept. 73-1V8-ARCPL-P1 (unpublished).

[4] Engelhardt, A. G., Phelps, A. V., and Risk, C. G., "Determination of Momentum Transfer and Inelastic Collision Cross Sections for Electrons in Nitrogen Using Transport Coefficients," *The Physical Review*, Vol. 135, No. 6A, Sept. 1964, pp. 1566–1574.

[5] Rapp, D. and Englander-Golden, P., "Total Cross Sections for Ionization and Attachment in Cases by Electron Impact," *The Journal of Chemical Physics*, Vol. 43, No. 5, Sept. 1965, pp. 1464–1479.

[6] Canavan, G. H., Proctor, W. A., Nielsen, P. E., and Rockwood, S. D., "CO_2 Laser Air Breakdown Calculations", *IEEE Journal of Quantum Electronics*, Vol. QE-8, June 1972, p. 564.

[7] Marquet, L. C., Hull, R. J. and Lencioni, D. E., "Studies in Breakdown in Air Induced by a Pulsed CO_2 Laser", *Digest of Technical Papers: VII. International Quantum Electronics Conference*, May 1972, p. 46.

[8] Smith, D. C. and Fowler, M. C., "Ignition and Maintenance of a CW Plasma in Atmospheric-Pressure Air with CO_2 Laser Radiation," *Applied Physics Letters*, Vol. 22, May 1973, pp. 500–502.

[9] Jackson, J. P. and Nielsen, P. E., "Role of Radiative Transport in the Propagation of Laser Supported Combustion Waves," *AIAA Journal*, Vol. 12, Nov. 1974, pp. 1498–1501.

[10] Edwards, A., Ferriter, N., Fleck, J. A. Jr., Winslow, A. M., "A Theoretical Description of the Interaction of a Pulsed Laser and a Target in an Air Environment", UCLR-51489, Nov. 1973, Lawrence Livermore Laboratory, Livermore, Calif.

[11] Nielsen, P. E. and Canavan, G. H., "Laser Absorption Waves in the Atmosphere," in *Laser Interactions and Related Plasma Phenomena*, Vol. 3, Plenum Pub., N.Y., 1974, pp. 177–189.

[12] Biberman, L. M. and Yakubov, I. T., "Approach to Ionization Equilibrium Behind the Front of a Shock Wave in an Atomic Gas," *Soviet Physics-Technical Papers*, Vol. 8, No. 11, May 1964, pp. 1001–1007.

[13] Sedov, L. I., *Similarity and Dimensional Methods in Mechanics*, 4th ed., Academic Press, New York, 1959.

[14] Raizer, Yu. P. "Heating of a Gas by a Powerfull Light Pulse," *Soviet Physics—JETP*, Vol. 21, No. 5, Nov. 1965, pp. 1009–1017.